SUPPLEMENTAL MATERIAL

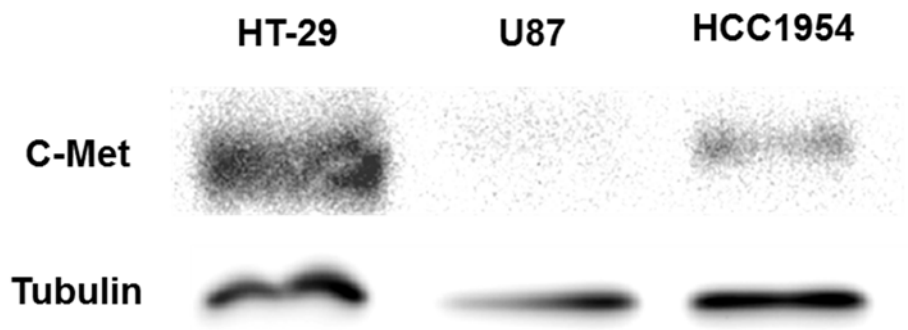

Supplemental Fig. 1. Western blot of c-Met expression. Highest expression level of c-Met is found in HT-29, less in HCC1954 and very little in U87 cell lysate. Tubulin was used as a loading control.

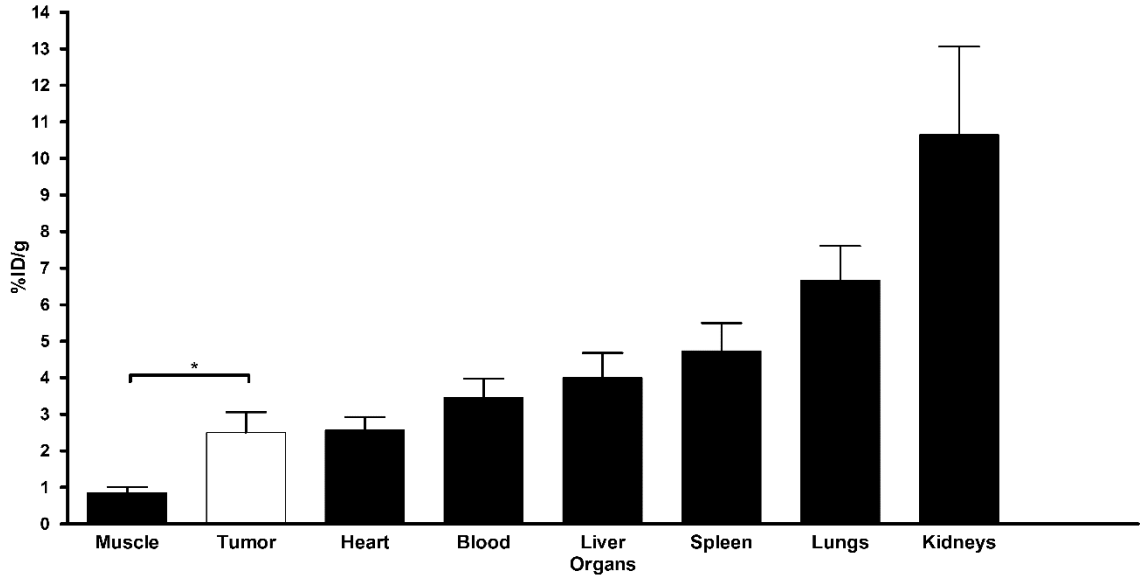

Supplemental Fig. 2. [^{18}F]AH113804 activity (% ID/g) from *ex vivo* assay of dissected organs and tissue samples from HCC1954 tumor bearing mice. Organs were excised at 70 min p.i. on Day 50 post tumor resection. A single *t*-test was performed to compare uptake of [^{18}F]AH113804 uptake in tumor and muscle. A statistically significant difference was observed ($p<0.05$, $n=3$). *P* value was calculated in R version 3.1.2.

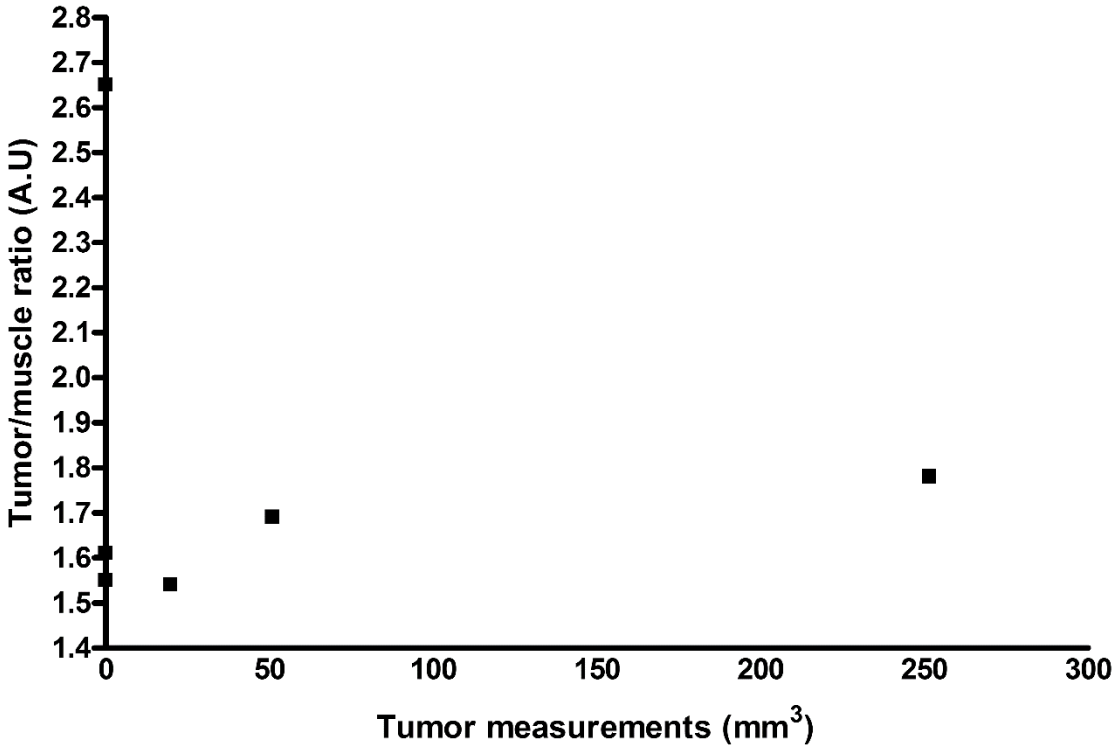

Supplemental Fig. 3. No correlation observed between tumor size by caliper measurement and the uptake of the tracer at the tumor site. This graph shows the mean tumour measurement of all tumour-bearing mice at 6 timepoints, with its matching mean uptake of the tracer (measurement taken at day 4 pre tumor resection, day 0, day 6, day 13, day 20, day 36 and day 50 post tumor resection).

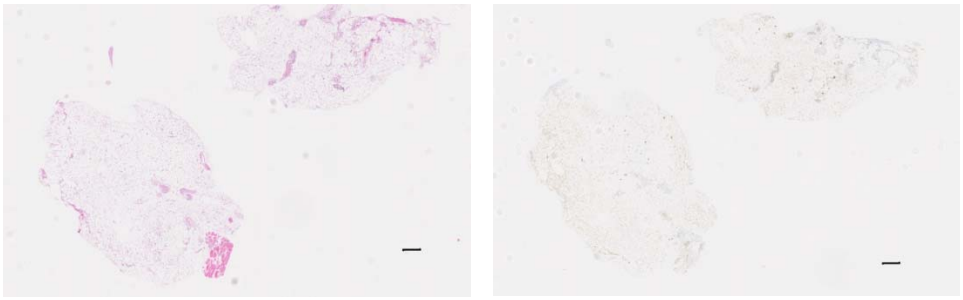

Supplemental Fig. 4. Immunohistochemical staining of mammary fat pad from a mouse that did not have a recurrent tumor after resection. The left panel represents the H&E staining of the sample that shows a clear presence of adipose tissue and ducts. No tumor cells were detected. The right panel shows staining for c-Met. No significant c-Met staining was observed. Scalebar represents 200 μm.

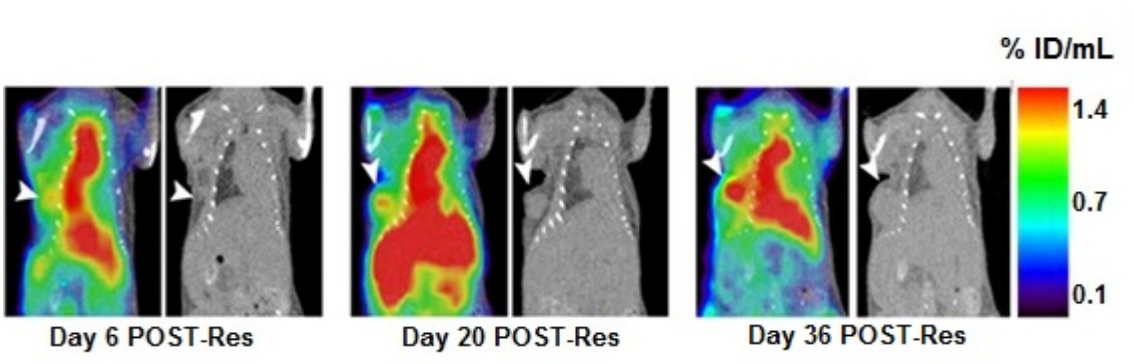

Supplemental Fig. 5. Progressive increase in uptake of [^{18}F]AH113804 at the tumor site post tumor resection. PET and CT image of a same tumor bearing mouse acquired on Day 6, Day 20 and Day 36 post resection showing uptake of [^{18}F]AH113804 at 60 min p.i. The recurrent tumour is clearly visible on the right flank of the animal (white arrowhead).

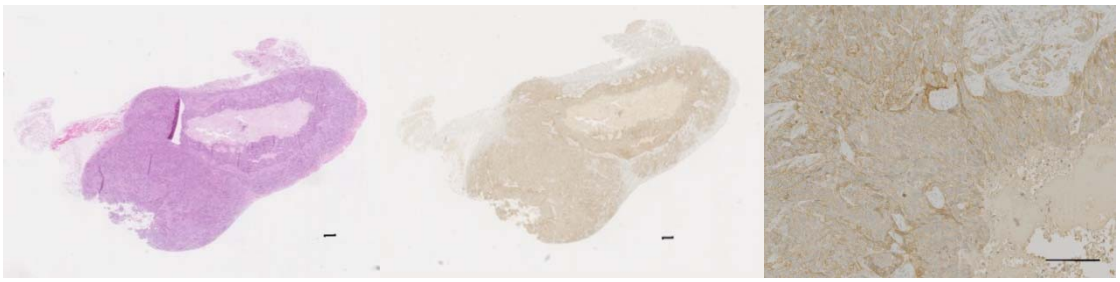

Supplemental Fig. 6. H&E staining E (left) and immunohistochemical staining for human c-Met (middle and right) on a representative tumour sample that was collected at day 14 post tumour inoculation. The tumour sample displays an area at its core devoid of cells. It also displays tumour cells at the periphery with fairly strong human c-Met staining. Presence of necrosis and membranous c-Met staining on tumor cells is visible on the right panel. Scalebars represent 200 µm.

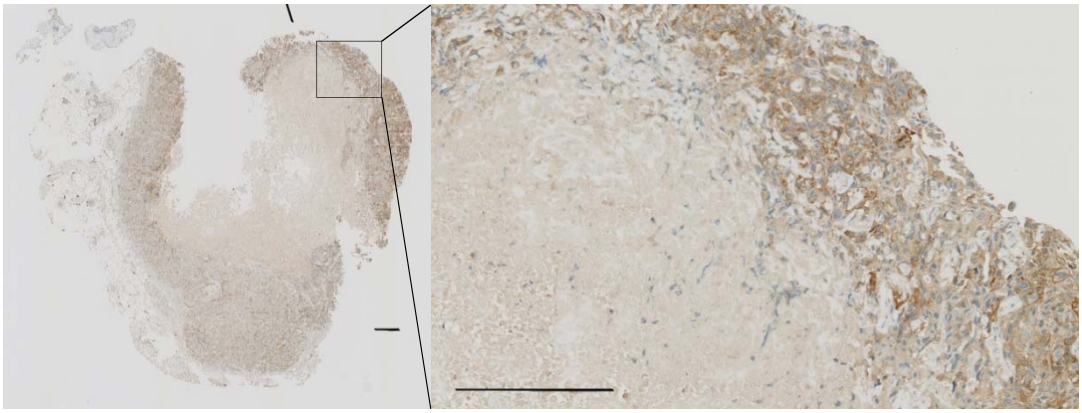

Supplemental Fig. 7. Immunohistochemical staining for c-Met on a representative recurrent tumor sample. Left panel shows the whole tumor sample while the right panel shows a magnified area of this tumor sample. The tumor sample displays a core of necrosis. The right panel shows membranous staining for c-Met around the tumor cells while the necrotic area shows no staining for c-Met. Scalebars represent 200 µm.

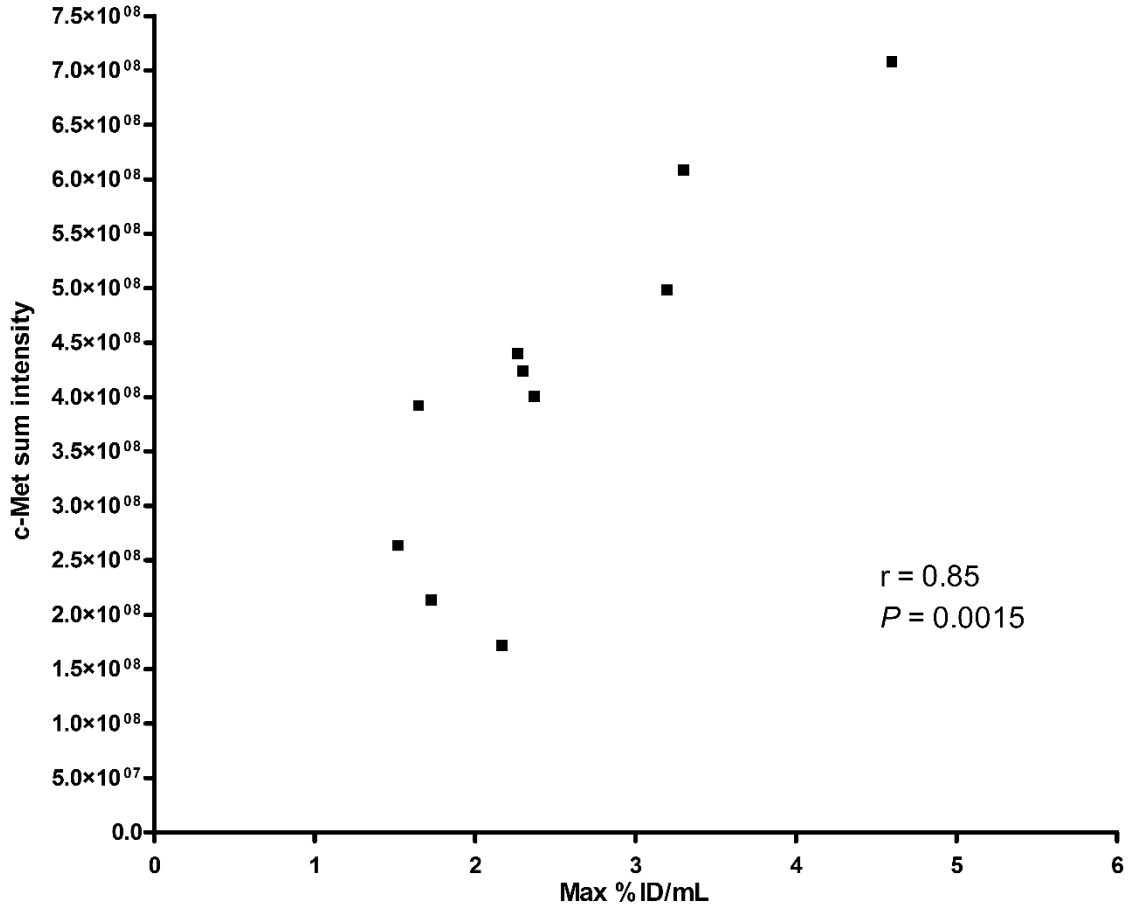

Supplemental Fig. 8. Uptake of [^{18}F]AH113804 in tumors correlates with the c-Met expression level in samples of the same HCC1954 tumors. IHC detection of c-Met expression in FFPE preparation of tumor samples. Statistical analysis gave a Pearson's correlation coefficient of 0.85 (*P*= 0.0015, n = 10). Pearson *r* and *P* values were calculated in R version 3.1.2.

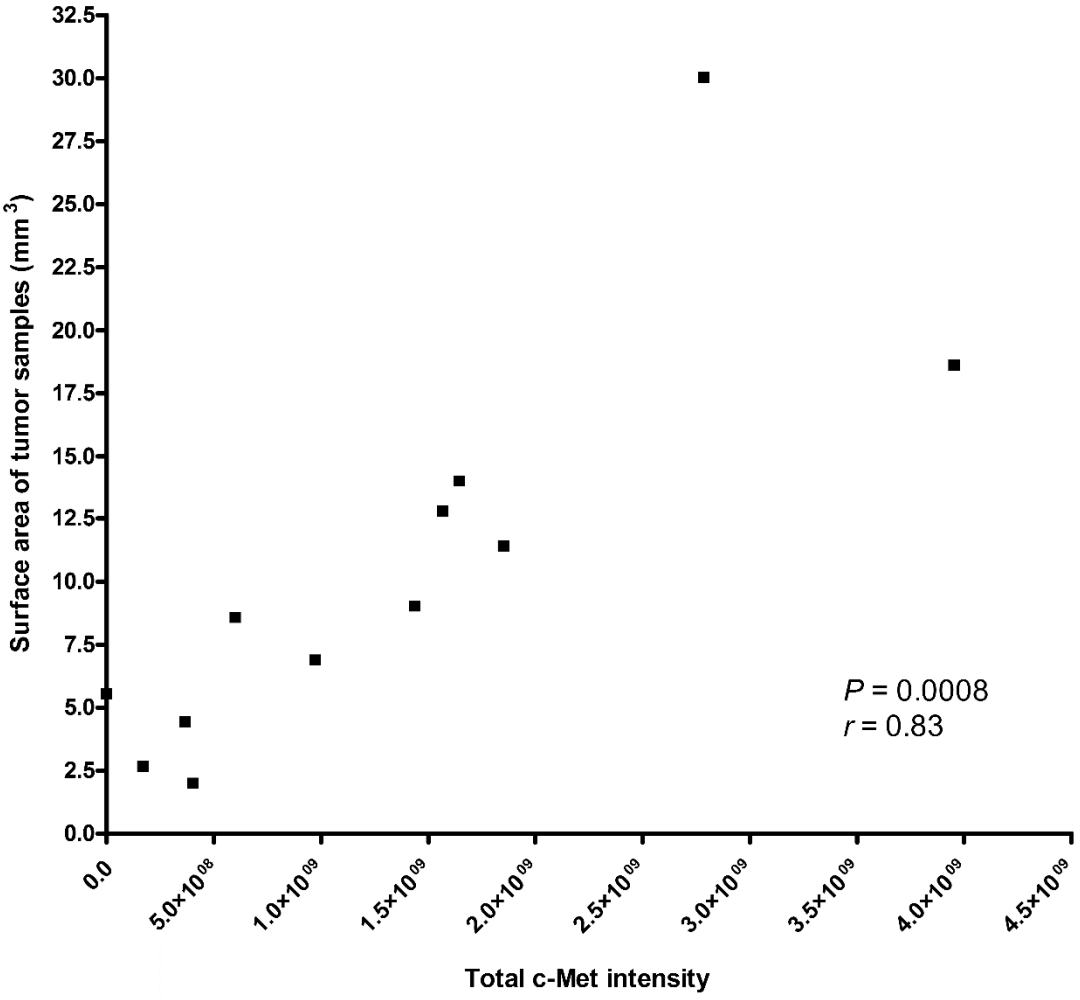

Supplemental Fig. 9. Correlation between the surface area of viable tumour cells and the total c-Met intensity. The surface area measured includes areas with tumour cells only while excluding areas without cells, necrotic areas, and stroma. Statistical analysis gave a Pearson's correlation coefficient of 0.83 (P = 0.0008, n = 12). P and r values were calculated in R version 3.1.2.

A B

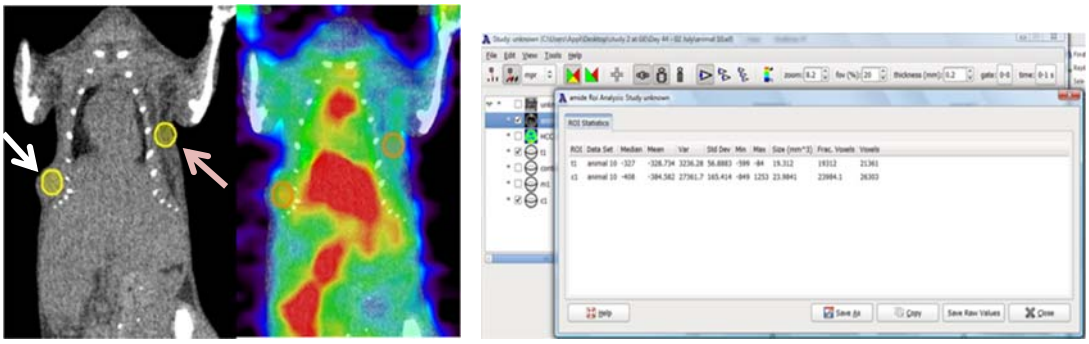

Supplemental Fig. 10. ROIs drawn in tumor and contralateral mammary fat pad. A. Representative CT (left) and CT/PET image (right) of HCC1954 tumour xenograft bearing mouse at day 36 post tumour resection. The ROI drawn at the tumour site (white arrow) was then replicated at the contralateral mammary fat pad (pink arrow) using the coronal and transverse section. **B.** ROI volumes for the tumour (t1) and the contralateral site (c1) are very similar. The ROI were drawn manually separately but attention was given to draw similar sized shape ROI for both sites and then checking that the volume of the respective ROI were very similar using the analysis section of the AMIDE software.

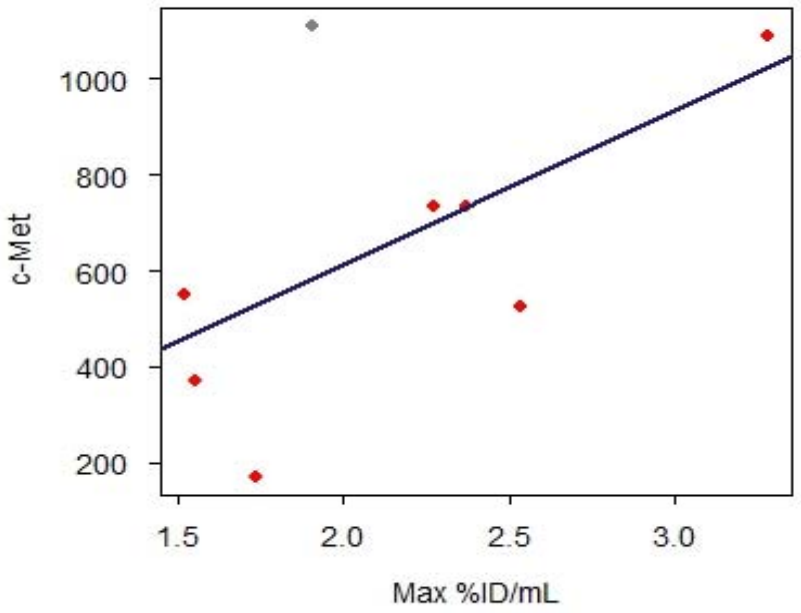

Supplemental Fig. 11. Identification of an outlier through the fitting of a regression line. Red dots fall between the upper and lower 1 percentile of all residuals while the grey dot is identified as an outlier. Statistical analysis performed in R version 3.1.2.

Day	MEAN (± SEM)	Lowest Individual Uptake Observed	Highest Individual Uptake Observed	n
-4	1.4 (0.2)	1.0	2.5	8
6	2.1 (0.1)	1.6	2.4	5
13	1.5 (0.2)	0.9	2.2	5
20	1.5 (0.3)	1.1	2.5	4
36	1.9 (0.7)	1.0	4.1	4
50	1.2 (0.3)	0.9	1.7	3

Supplemental Table 1. Uptake of radioactivity (%ID/mL) in HCC1954 tumors following [^{18}F]AH113804 administration, as determined by PET imaging.

PET Imaging timepoint	Number of mice imaged	Number of mice with recurrent tumors
10 days post implantation	8	N/A
6 days post resection	8	5
13 days post resection	8	5
20 days post resection	6	4
36 days post resection	6	4
50 days post resection	6	3

Supplemental Table 2. Number of mice used in this study and imaged at different PET imaging timepoints. Inclusion of the number of mice with visible recurrent tumors after tumor surgery.

Supplemental Methods:

Tumor xenograft model (continuation):

Initial PET scans with [^{18}F]AH113804 were acquired 10 days after tumor inoculation. Fourteen to sixteen days after tumor cell implantation, animals underwent surgery for tumor excision, and were subsequently allowed to recover under sufficient analgesia.

The animals were anaesthetized using 2.5% isofluorane in medical oxygen during the surgery. Area of the tumor site was cleaned using povidone-iodine. A 1 cm incision was then made around the tumor. A cotton swab was used to expose the tumor from the mammary fat pad. The tumor was then removed gently and completely from the mammary fat pad using scissors. In some cases, when the tumor was stuck to the skin, the skin was also removed to ensure that there would be no visible remnant of the tumor. Sham surgery was not performed on the contralateral mammary fat pad as the project license would not allow 2 surgeries to take place in one animal.

The animals were monitored for up to 50 days post tumor resection for local tumor recurrence, with PET imaging carried out on selected days post resection (Suppl. Table 2).

For autoradiography studies, female nude mice were inoculated with HC1954 cells in the second right mammary fat pad, according to the methods described above. Tumors were allowed to develop for 25 days before use.

Radiosynthesis of [^{18}F]AH113804 (continuation):

[^{18}F]AH113804 (chemical structure presented in Fig. 1A) was synthesized on a FASTlab automated synthesizer (GE Healthcare, Chalfont St Giles, UK) in a 2-step process. First, [^{18}F]fluorobenzaldehyde was synthesized from [^{18}F]fluoride and purified on a MCX+ (Mixed Cation Exchange, Waters) cartridge. Then, [^{18}F]fluorobenzaldehyde was conjugated to the peptide precursor and [^{18}F]AH113804 was purified and formulated.

[^{18}F]Fluoride was recovered from irradiated target water on a QMA cartridge (Waters) and then eluted using Kryptofix and $KHCO_3$ into a cyclic olefin copolymer reaction vessel and dried under a flow of

nitrogen at 120 °C. Subsequent reaction with trimethylammonium benzaldehyde triflate in DMSO resulted in [^{18}F]fluorobenzaldehyde.

In the second step, the peptide precursor was dissolved in an aqueous solution of aniline hydrochloride and added to the purified [^{18}F]fluorobenzaldehyde to give crude [^{18}F]AH113804. Purification was done on a tC18 SPE (Solid Phase Extraction) cartridge with acetonitrile in PBS (21.4% v/v) followed by PBS to remove residual acetonitrile. [^{18}F]AH113804 was eluted into PBS (34 mL) from the tC18 cartridge with ethanol (2.4 mL) followed by PBS (2.6 mL) to give the formulated product (total volume 39 mL, ca. 6% EtOH).

CT and PET imaging:

Anesthesia (approximately 2% isoflurane in oxygen) was induced shortly before and maintained throughout imaging. PET imaging at 55-65 min post injection (pi) of [^{18}F]AH113804. A whole body CT scan followed (projection exposure time 400 ms, tube voltage 45 kVp). Animals were allowed to recover from anesthesia. Occasionally static PET imaging was replaced by a dynamic series at 5-65 min pi [^{18}F]AH113804.

PET data were attenuation and scatter corrected, then reconstructed by filtered back projection. Images were manually coregistered and analyzed by Regions of Interest (ROI) employing AMIDE (http://amide.sourceforge.net).

Imaging was performed at baseline (10 days post tumor inoculation, i.e. 4 days pre-resection) and on Days 6, 13, 20, 36 and 50 post tumor resection.

3D ellipsoid ROIs were placed on the tumor in CT images to estimate tumor volume (Suppl. Fig. 10). Additional ROIs were placed in skeletal muscle (left forelimb), liver, left and right kidney, and heart (blood pool). All ROI PET data were expressed as decay corrected radioactivity concentration normalized to the injected dose (% ID/mL).

Biodistribution of [^{18}F]AH113804 was obtained for the mice on the final imaging day (Day 50 post resection). Following PET/CT imaging, animals were sacrificed (approx. 70 min p.i.). Organs and tissues of interest were excised, weighed and radioactivity measured using a custom-built twin-crystal gamma counter. Ex vivo [^{18}F]AH113804 uptake is expressed as percentage radioactive dose per gram of tissue (% ID/g).

Autoradiography:

Autoradiography was performed on tumors harvested from nude mice 25 days after tumor inoculation. Mice were sacrificed 40 min after injection of approximately 7 MBq [^{18}F]AH113804 and corresponding PET imaging. Tumors were excised, snap frozen and cut into 8 µm thick sections. Sections were then imaged in a Micro Imager (Biospace Lab, Paris) which provides a spatial resolution of 25 µm for ^{18}F. Image acquisition duration was 90 min.

Histology:

Hematoxylin and eosin staining and c-Met immunohistochemistry were performed on consecutive 3µm thick tissue sections, employing the monoclonal rabbit antibody D1C1 (Ventana; diluted 1:30) against total c-Met. Antigen retrieval was employed (Standard Cell Conditioning 1/ Ventana). DAB (3,3'-diaminobenzidine) served as chromogen. Slides were processed with an automated system Ventana (BenchMark ULTRA, Roche, Switzerland), scanned with a Hamamatsu Nanozoomer 2.0 HT (Hamamatsu Photonics, Hamamatsu, Japan) and initially analyzed with Hamamatsu NDP.view2 viewing software. Quantitative analysis of the c-Met expression level was made using HistoQuest 4.2 (Tissugnostic, Vienna, Austria) software. IHC detection and quantification of c-Met expression in FFPE preparation of tumor samples are described in the section below.

Immunohistochemistry Data Analysis:

All the histological slides were digitalized at magnification x20 (0.46 µm/pixel) using Hamamatsu Nanozoomer 2.0 HT. Digital images in ndp format were submitted for quantitative image analysis using HistoQuest software. HistoQuest uses patented algorithms to detect the individual cells of interest and assesses intensity of antigens in the cell nucleus, membrane and cytoplasm. The program automatically detects tissue which is subjected to color separation module to differentiate between the blue and the brown shade. Nucleus detection algorithm on the hematoxylin shade was used to detect all cell nuclei and was defined as master channel. A ring mask around each nucleus was used to analyze the staining intensity of

non-master chromogen (DAB) in given cellular location. The staining intensity is measured as mean intensity of all pixels of a cell and the range of values is from 0 to 255.

c-Met staining intensity was analyzed within 1.7 mm² regions of interest (ROI) that were visually identified over the tumor enriched region. Staining intensity was analyzed in ring masks around each nucleus using an algorithm that identifies stained cytoplasmic and membranous areas. Raw data included minimum and maximum pixel value for every individual cell within the ROI. The average minimum and maximum pixel values were calculated for the whole region. The obtained data correlated with values acquired from PET scans.

Immunofluorescence:

Tissues were permeabilized and stained similar to the procedure outlined previously (*18*). A monoclonal rabbit c-Met antibody (1:100, D1C2, Cell signaling), followed by an incubation with a goat anti-rabbit Cy3 secondary antibody (1:500, Sigma), were used. Total fluorescence in each sample was measured and total c-Met-related intensity was corrected for differences between each animal using the same threshold. It was quantified using the software package TRI2 (Paul Barber, Oxford Institute for Radiation Oncology).

Statistical Analysis:

SEM was calculated to estimate the precision of the sample mean. Paired *t*-test of log-transformed TMRR was conducted to evaluate the difference between tumor and contralateral mammary fat pad uptake (Fig 2B). The correlation between total c-Met intensity from frozen tumor samples and the corresponding max %ID/mL for the uptake of [^{18}F]AH113804 at the tumor site (Fig 6B) is visualized with a scatter plot and Pearson correlation coefficients were calculated. The analysis was restricted to observations which fell between the upper and lower 5 percentile of all residuals, assigning any observation beyond this range as an outlier. This resulted in exclusion of one observation and the remaining seven observations were used in the final analysis (Suppl. Fig. 11). A two-sided P-value <0.05 was used to determine significance.